

# A novel gelatin sponge for accelerated hemostasis

Reiner Hajosch,<sup>1</sup> Markus Suckfuell,<sup>2</sup> Steffen Oesser,<sup>3</sup> Michael Ahlers,<sup>4</sup> Klaus Flechsenhar,<sup>4</sup> Burkhard Schlosshauer<sup>1</sup>

<sup>1</sup>NMI Natural and Medical Sciences Institute, University of Tübingen, Reutlingen D-72770, Germany

<sup>2</sup>Department of Oto-Rhino-Laryngology, University Medical Centre, Ludwig-Maximilians-University, Munich, Germany

<sup>3</sup>Collagen Research Institute, University Campus at Kiel, Germany

<sup>4</sup>GELITA AG, D-69412 Eberbach, Germany

Received 23 December 2009; revised 2 March 2010; accepted 3 March 2010

Published online 24 June 2010 in Wiley InterScience (www.interscience.wiley.com). DOI: 10.1002/jbm.b.31663

**Abstract:** To more effectively manage the substantial bleeding encountered during surgical procedures in oto-rhino-laryngology, we developed a novel hemostatic sponge made of pharmaceutical grade, chemically cross-linked gelatin. The sponge is characterized by a high pore density, reduced ligaments, and a high nanoscale roughness of lamella surfaces in the matrix. *In vitro* blood uptake assays revealed a very rapid absorption of human blood, which was two to three times faster than that measured with comparative hemostytic devices. In an *in vitro* hemorrhage model using human veins, the novel gelatin sponge matrix induced hemostasis less than a minute after bleeding was induced. The sponge was shown to bring about rapid hemostasis when it was administered in a young patient suffering from acute bleeding of a pharyngeal angiofibroma, even though the patient

had been treated with an anticoagulant because of a transient ischemic attack. As the gelatin matrix of the sponge is biocompatible and resorbable, the hemostytic device could be left in place and was shown to be resorbed within 2 weeks. We hypothesize that the excellent hemostatic performance of the sponge might be linked to enhanced capillary effects in conjunction with optimized anchoring of fibrinogen on the nano-rough material surface, as suggested by scanning electron microscopy. The novel gelatin sponge appears to be a promising hemostatic matrix, which could be of great benefit for patients suffering from epistaxis and other acute injuries resulting in severe bleeding. © 2010 Wiley Periodicals, Inc. *J Biomed Mater Res Part B: Appl Biomater* 94B: 372–379, 2010.

**Key Words:** absorbable, blood, gelatin, hemostasis, sponge

## INTRODUCTION

Uncontrolled bleeding after traumata or after surgical interventions is a major cause of morbidity and mortality. Basic emergency treatment typically includes the application of absorbent dressings in conjunction with pressure, binding, and tourniquets to acutely stop bleeding. In the majority of cases, the hemostatic effect is probably based on the latter physical measures rather than on the nature of the dressing. Although considerable efforts have been made to develop more advanced wound dressings, the current spectrum of products and procedures is far from satisfactory for the multitude of medical needs, including closure of arteriotomies,<sup>1</sup> joint arthroplasty procedures and bone resection following hypertrophic growth,<sup>2</sup> acute epistaxis, functional endoscopic sinus surgery, turbinoplasty,<sup>3</sup> and many others.

The development of more advanced dressings must take into consideration different material types and modes of action. Classic absorbent dressings neither initiate nor potentiate platelet activation or clot formation. Cotton gauze pads and starch-based powders traditionally belong to this group. In contrast to absorbents, hemostats actively stop bleeding either by (a) coagulation enhancement, (b) platelet activation, or (c) an unknown mechanism. (A) Presently

available coagulant-enhancing dressings actively generate fibrin. To achieve efficacy in that regard, glycan or freeze-dried collagen is doped with thrombin and fibrinogen.<sup>4–6</sup> To be even more effective, some thrombin-fibrinogen dressings additionally incorporate inhibitors of fibrinolysis, such as aprotinin.<sup>7</sup> (B) Alternatives to coagulants are dressings that enhance platelet effects. Collagen and some collagen derivatives have been demonstrated to either activate platelets or stimulate their aggregation.<sup>8</sup> (C) This group of hemostatic dressings includes medical devices with outstanding absorbent properties including anhydrous granular zeolite (crystalline aluminosilicate).<sup>9–12</sup> It should be noted that this material displays its hemostatic potency only in the dry state. Sealants could also be added to the list of dressings, although their action is—strictly speaking—dependent on a purely passive mechanism. Sealants are impermeable barriers, for instance forming gelatinous plugs; these are usually based on acetylated or deacetylated poly-*N*-acetylglucosamine or chitosan derivatives. Cyanoacrylates and self-assembling peptides belong to the more recently developed sealants.<sup>13,14</sup>

Amongst the many different techniques available (e.g., surgical treatment or embolization)<sup>15</sup> nasal packing is a

**Correspondence to:** B. Schlosshauer; e-mail: schlosshauer@nmi.de  
Contract grant sponsor: BMBF (German Ministry of Education and Research)

common method of handling epistaxis. Although the benefit of nasal packing is currently a matter of controversy,<sup>16,17</sup> absorbable hemostats could bring major improvements, as they obviate the removal of nasal packs and improve patient comfort.<sup>18</sup>

Stimulated by the medical need for more advanced curative interventions in minimally invasive as well as in otolaryngological surgery where substantial bleeding can be expected, for example, after angiofibroma resections and turbino-plasty,<sup>19</sup> we began to develop a hemostatic, gelatin-based sponge that is devoid of further additives, such as fibrinogen, thrombin, or related fibrinogenic pharmaceuticals.

## MATERIALS

PBS was obtained from PAA Laboratories (Pasching, Austria), isopropyl alcohol, PFA, and sodium chloride from Carl Roth (Karlsruhe, Germany), sucrose from Sigma-Aldrich (Taufkirchen, Germany), and glutaraldehyde from Merck (Darmstadt, Germany). The two different sponge types (see Figure 1) GelitaSpon<sup>®</sup> and X-sponge were provided by Gelita AG (Eberbach, Germany).

## METHODS

### Hemostyptic sample processing

For the production of the novel hemostyptic sponge (technical term: X-sponge or X-BLOND<sup>®</sup>) a purified fraction of pharmaceutical grade gelatin from pig skin was used. The gelatin solution was air-bubbled in the presence of a chemical cross-linker; dried and mechanically processed (details are the subject of ongoing patent proceedings). Sterilization was performed by gamma irradiation. Sponges were used for analysis either in a dry state or after prior hydration (dipping into PBS, 5 s) and subsequent slight compression to remove excess fluid.

### Electron microscopy/histology

For ultrastructural analysis, specimens were rapidly fixed in 4% paraformaldehyde (PFA, 2d, 4°C) and subsequently in 2% glutaraldehyde/PFA (5d, 4°C), washed in phosphate-buffered saline (PBS), and critical point dried in isopropyl alcohol (eight cycles) to remove traces of water. Before scanning electron microscopy (Zeiss microscope DSM 950), the samples were sputtered with palladium/gold (20/80). Specimens w/o blood were processed immediately after the experiments were finished. For semiquantitative evaluation five regions of interest (ROI) from three samples each were defined. A virtual grid with three horizontal and three vertical equidistant lines was superimposed onto each ROI. All lamellae/ligaments of the gelatin sponge and pores positioned on these lines were measured using the software ImageJ 1.41 (<http://rsbweb.nih.gov/ij/>) (GelitaSpon:  $n = 432$ ; X-sponge:  $n = 607$ ). For statistical analysis the software Statview 5.0 (SAS Institute, North Carolina, USA), ANOVA, and Mann-Whitney tests were used. Samples with  $p < 0.001$  were considered to be statistically highly significant.

To visualize blood-binding profiles on sponge specimens, human blood from informed healthy volunteers was collected without anticoagulant. Postoperative testing revealed

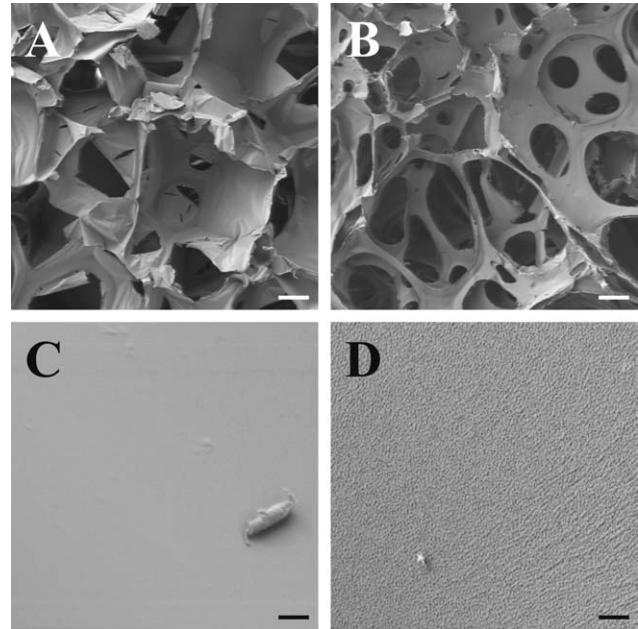


**FIGURE 1.** Gelatin sponges. Scanning electron micrographs of hemostatic gelatin sponges of a control specimen (A) and X-sponge (B). X-sponge displayed narrower lamellae and a somewhat higher porosity. High magnifications of the gelatin lamella surfaces of a control specimen (C) and X-sponge (D). The control specimen displays a smooth surface, X-sponge a roughness on a nanoscale. Scale bars: (A, B) 100  $\mu\text{m}$ , (C, D) 1  $\mu\text{m}$ .

values in the normal range for INR, PTT, and fibrinogen. The experiment was run immediately after drawing blood, following the blood uptake assay protocol. Afterward the resulting blood-soaked hemostatic sponges were processed for electron microscopy and histological staining as described above.

For histological staining, PFA-fixed samples were impregnated with 30% sucrose/PBS (4d, 4°C) and subsequently immersed in Tissue Tek<sup>TM</sup> O.C.T. Compound (Sakura, Torrance, Canada), frozen in liquid nitrogen and cryosectioned (10  $\mu\text{m}$  sections). Sample sections were mounted on SuperFrost<sup>®</sup> glass slides (Menzel, Braunschweig, Germany) and stained with hematoxylin-eosin (Merck, Darmstadt, Germany). Stained sections were evaluated with an inverted microscope (Axiovert, Zeiss, Oberkochen, Germany) and digitally documented using the AxioVision4.6 software program (Zeiss).

### Blood absorption assay

Human erythrocyte concentrate stabilized with CPD/SAG-M (UKT, Tübingen, Germany) was allowed to reach ambient temperature. Isotonic saline solution was added (1:4 dilution) resulting in a hematocrit of 40–56%. The blood absorption capacity of each sample was measured in triplicate. The sponge material (5 × 1 × 3 cm) was smoothly applied onto the blood surface for 20 s. Then the blood soaked sponge was immediately placed on one filter layer (MN 615, Macherey-Nagel, Düren, Germany) for 60 s to remove superficial blood. The sponge weight was measured with a microscale (Mettler AE 166, Mettler Toledo, Giessen,

Germany) before blood contact ( $M_d$ ) and after removing surplus surface blood via the filter layer ( $M_w$ ). Blood absorption capacity was calculated according to the following formula:

$$\text{blood absorption capacity} = \frac{M_w - M_d}{M_d}$$

### Blood uptake assay

Human erythrocyte concentrate preparation was performed as described in the blood uptake assay (see above). For the blood uptake assay, a glass plate was positioned at an inclination of 25° in a circular container (Ø 8 cm). The test hemostatic sponge (2 × 1 × 5 cm) was positioned on the glass plate and 6 mL blood was filled into the container. Over a 5-min period, the upward migration of the blood front (expressed as distance from the original blood level) was measured every 30 s.

### Hemorrhage model *ex vivo*

To test the hemostatic efficacy of X-sponge, a dynamic hemorrhage model was used (publication in preparation). Briefly, to simulate diffuse venous bleeding human varicose veins (V. saphena magna) were obtained after phlebectomy. The veins were refilled with autologous heparinized blood (2.5 IU/mL) and connected to a blood pressure manometer. Blood pressure was adjusted to normal venous pressure of 30 mm Hg. At the beginning of the experiment defined vessel leakage was initiated by puncturing the vein with a 14-gauge needle. To stop bleeding the tested hemostyptic of a defined size (10 mm × 10 mm) were applied directly to the laceration. Then elapsed time was measured until complete hemostasis was achieved. To quantify blood loss the blood leaking out of the wound was collected and the total amount was determined. The hemostatic efficacy of X-sponge was tested in comparison with a standard gelatine sponge (GelitaSpon®). GelitaSpon® was used as per the manufacturers' instructions after moistening the sponge with saline solution, whereas the X-sponge was used in a dry or premoistened state.

### Human application

The application of X-sponges in humans was initially classified and approved as an "individueller Heilversuch" (individual medical treatment without defined protocol). In the meantime X-sponges have been CE-certified as X-BLOOD®. The motivation for using the novel X-sponge in a small number of selected patients was to gain clinical experience with the hemostyptic sponge in ENT patients (ENT: ear, nose, and throat). We collected data, for example, from patients who either presented to the ENT department for the emergency treatment of epistaxis or who were selectively operated for the treatment of adenomas or sinusitis with functional endoscopic sinus procedures or turbinoplasties. A number of patients when presenting to the ENT department had been treated with anticoagulants, such as aspirin, clopidogrel, or coumadine.

## RESULTS

### Gelatin sponge microstructure

For the sake of simplicity, the novel gelatin sponge will be designated X-sponge to allow convenient distinction from other specimens. X-sponge was produced by chemical cross-linking of purified pharmaceutical grade gelatin and subsequent technical processing, which included oriented compression (details are the subject of ongoing patent proceedings). Scanning electron microscopy revealed that the X-sponge was characterized by a more elaborate pore system than the standard gelatin sponge (GelitaSpon®), which is approved for human application. Images (200× magnification) of X-sponge suggested smaller lamellae and a higher porosity [Figure 1(A,B)]. The lamellae of X-sponge often narrowed down to tight trabeculae, whereas the standard sponge displayed expanded interconnecting lamellae. Higher magnification (20,000×) revealed that the standard sponge had a smooth surface, in contrast to the X-sponge with its consistent surface roughness in the nanorange [Figure 1(C,D)]. For quantitative evaluation, five areas from a given sample were used for electron microscopy. The resulting scanning micrographs (200×) were overlaid with a 16-field grid, and the lamellae and pores lying on horizontal or vertical grid lines were quantified [Figure 2(A)]. The percentile diagram for the distribution of lamellae [Figure 2(B)] clearly indicated that there were significant differences between the two types of sponges (Mann-Whitney test,  $p < 0.001$ ). As depicted in Figure 2(C), X-sponge had smaller pores and its lamellae covered a smaller area on the average. Because of the high sample number (>400), the differences were calculated to be highly significant ( $p < 0.001$ ). When we calculated the ratio of average pore diameter to average lamella size, we found that the X-sponge had a porosity 1.3 times higher than that of the standard sponge.

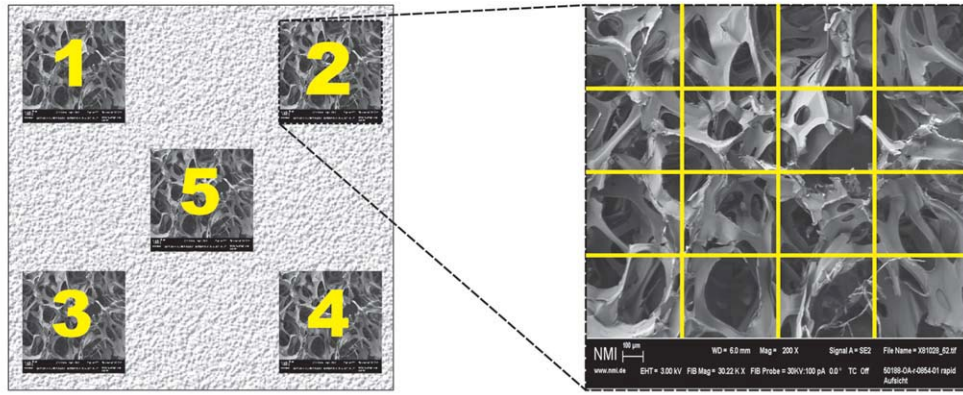
### Blood absorption/uptake *in vitro*

**Blood absorption.** When dry X-sponge was exposed to fluid, we found that the sponge absorbed 40 times its own weight. The blood absorption capacity of X-sponge in a dry state was calculated to be 58 g blood per g sponge material, whereas the standard sponge showed a blood absorption capacity of 1 g blood per g material (Figure 3).

**Blood uptake.** To quantify the time course of blood uptake, diluted human erythrocyte concentrate was used in a specially designed device [Figure 4(A)]. In this device test sponges were positioned on a glass plate of defined inclination situated in a container filled with a small amount of blood. After 300 s, blood stopped wicking at a height of 3.2 cm in the case of dry X-sponge [Figure 4(B)]. Prehydrated X-sponge was slightly less effective (2.9 cm). This was in pronounced contrast to the hydrated control sponge displaying a blood migration distance of only 0.9 cm. Non-prehydrated (dry) control sponges showed no uptake. The quantitative data were supplemented by qualitative cytochemistry. Specimens used for the above quantitative assays were fixed, cryosectioned and subsequently stained. Hematoxylin-eosin staining illustrated that blood uptake was

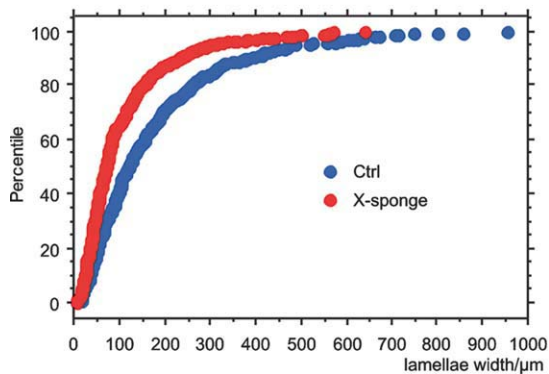
## Principle of image analysis

A



B

### Lamellae of different sizes



C

### Averages of lamellae /pores

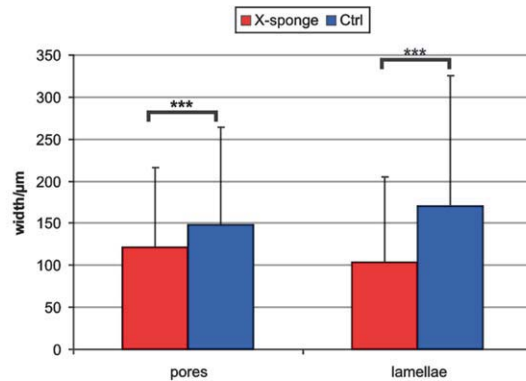
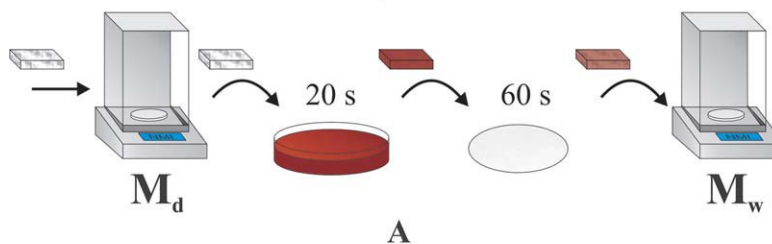


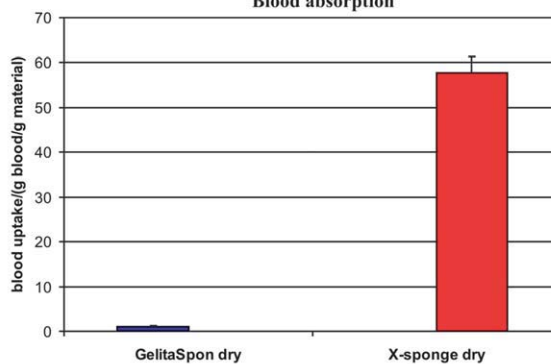
**FIGURE 2.** Image analysis of gelatin sponges. Scanning electron micrographs of hemostatic gelatin sponges of a control specimen and X-sponge were evaluated by image analysis. Five areas from a given sample were overlaid with a grid pattern and lamellae and pores positioned on grid lines were quantified (A). Percentile diagram of lamellae shows a significant difference in size distribution between the two sponge types (Mann-Whitney,  $p < 0.001$ ) (B). Comparison of pores and lamellae (C). X-sponge has smaller pores and lamellae (GelitaSpon:  $n = 432$ ; X-sponge:  $n = 607$ ,  $***p < 0.001$ , SE). [Color figure can be viewed in the online issue, which is available at [www.interscience.wiley.com](http://www.interscience.wiley.com).]

### Assay scheme



A

### Blood absorption



B

**FIGURE 3.** Blood absorption capacity *in vitro*. Scheme of the experimental layout (A). Test sponges were positioned on the surface of diluted human blood cell concentrate for 20 seconds. Surplus blood was eliminated on a paper filter for 60 seconds. Masses of dry sponges ( $M_d$ ) and blood-soaked sponges ( $M_w$ ) were determined. In a dry state the blood absorption capacity of X-sponge is 58 times higher than that of the control sponge (B). [Color figure can be viewed in the online issue, which is available at [www.interscience.wiley.com](http://www.interscience.wiley.com).]

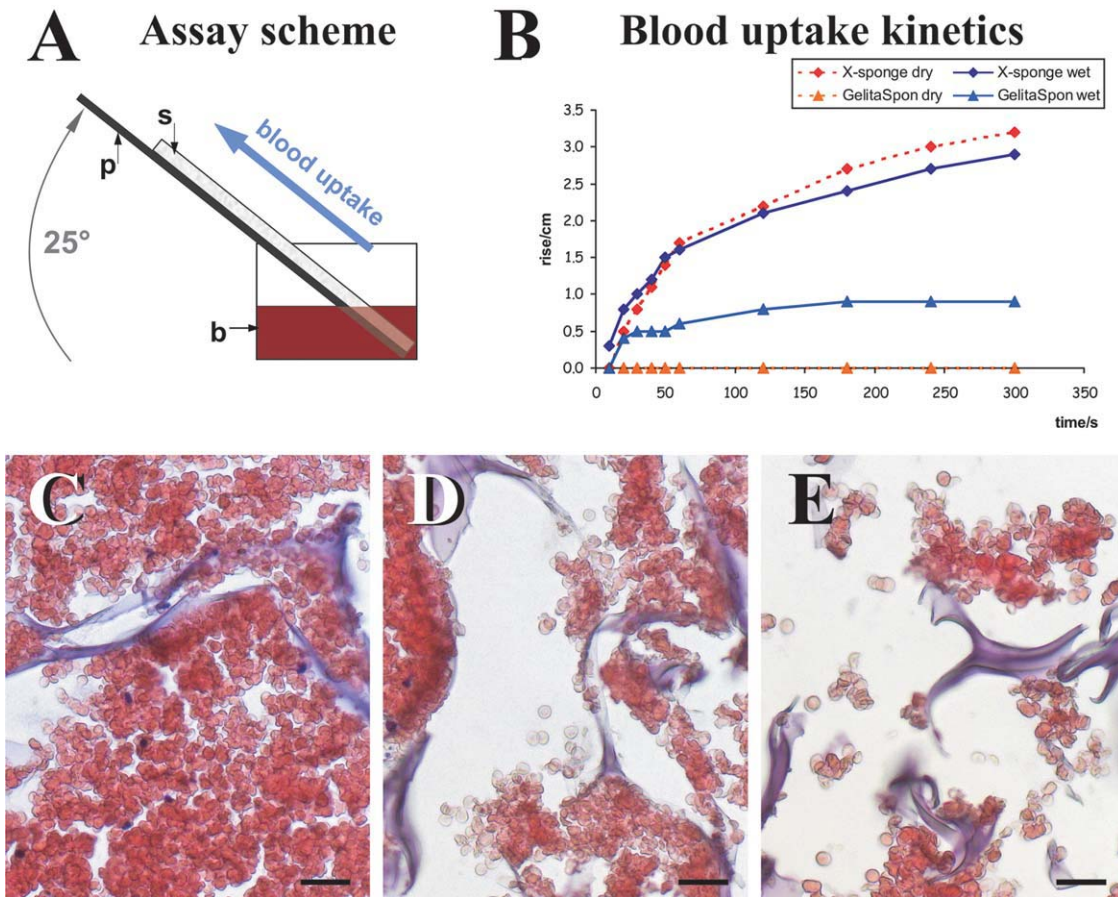


**FIGURE 4.** Blood uptake *in vitro*. Scheme of the experimental layout (A); b, blood substitute = adjusted human blood cell concentrate; p, plate; s, sponge. Test sponges were positioned on a glass plate (25° inclination) placed in a container partially filled with diluted human cell concentrate. The position of the leading blood margin was determined at different time points and graphically depicted (B). Micrographs of hematoxylin-eosin stained cryosections of sponge specimens after blood uptake of blood (C–E). Bottom region (about at 5 mm) (C), intermediate region (about at 20 mm) (D), and top region (about at 40 mm) (E). A gradient of cells is evident from the bottom to the top, but no fractionation of cells of different sizes. Scale bar: (C–E) 50  $\mu\text{m}$ . [Color figure can be viewed in the online issue, which is available at [www.interscience.wiley.com](http://www.interscience.wiley.com).]

characterized by a gradient of blood cells with the highest density at the bottom, where essentially all cavities were filled with erythrocytes [Figure 4(C)]. In the middle of the sponge [Figure 4(D)] cavities were partially filled with cells. Toward the top of the sponge, cavities were essentially cell-free [Figure 4(E)]. Despite the cell-density gradient, we had no indication of a chromatographic effect with obvious signs of a separation of small and large cells.

Electron microscopic analysis revealed that the blood cells (predominantly erythrocytes) appeared in close apposition to the gelatin lamellae, irrespective of the type of sponge [Figure 5(A,B)]. Depending on the actual site selected for electron micrographic inspection, the density of observed cells varied and could not be correlated to the sponge microstructure at low magnification (800 $\times$ ). However, high magnification (10,000 $\times$ ) images clearly suggested that the X-sponge lamellae were coated by a multitude of submicron profiles of irregular shape and by filament-like structures several 10 s of micrometers in length resembling fibrin fibers [Figure 5(D)]. Control sponges also displayed a fibrin network with embedded erythrocytes, but appeared to

have a less pronounced submicron profile [Figure 5(C)]. The images could indicate an increased number of fibrin attachment sites on X-sponge gelatin surfaces (see discussion).

#### Homeostasis *ex vivo*

In a novel dynamic venous hemorrhage model, the hemostatic efficacy of X-sponge was evaluated in comparison with the standard hemostyptic material, GelitaSpon<sup>®</sup> [Figure 6(A)]. Human saphenous veins were mounted in a pump and pressure monitoring system. A continuous flow of autologous heparinized blood was maintained. The vein was lacerated to create a leak in the vessel. Bleeding time and blood loss was measured after application of the hemostyptic devices. In our hemorrhage model, adequate hemostatic efficacy was observed after application of GelitaSpon<sup>®</sup>. Surprisingly, the hemostyptic effect of dry X-sponge was more than double that of GelitaSpon<sup>®</sup>, as indicated by a significant reduction in the determined bleeding time (–62.5%) and a reduced blood loss (–67.8%) after laceration [Figure 6(B,C)]. In additional experiments no significant differences between moistened and dry X-sponges became evident.

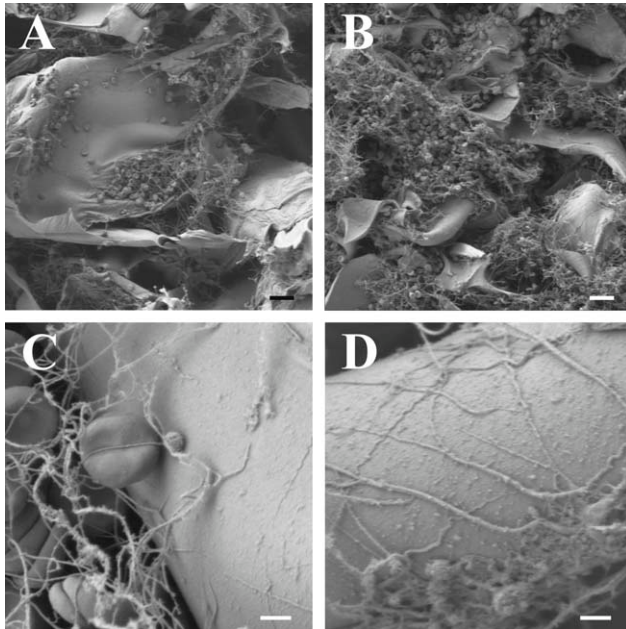


**FIGURE 5.** Blood-binding profiles on sponge surfaces. Scanning electron micrographs of gelatin sponges of a control specimen (A, C) and X-sponge (B, D) after blood uptake w/o anticoagulant *in vitro*. Low (A, B) and high magnifications (C, D). For both sponges an accumulation of blood cells is evident (A, B). High magnifications of the gelatin lamellae of a control specimen with a fairly homogeneous surface (C) and X-sponge with blood-binding profiles partially in conjunction with fibrin-like fibers (D). Scale bars: (A and B) 20  $\mu\text{m}$ , (C and D) 2  $\mu\text{m}$ .

### Human application

X-sponge was used in an emergency situation involving a 12-year old male, who presented to the medical center with acute bleeding. He was diagnosed with a pharyngeal angiofibroma which extended into the left paranasal sinus, the right pterygopalatine fossa and the right sphenoid sinus with contact to the right maxillary sinus. After admission, the young patient underwent selective arterial angiography [Figure 7(A)] to visualize the vascular structure of the tissue mass, followed by embolization. Unfortunately, a small portion of the embolisate reached the internal carotid artery, resulting in neurological symptoms, such as recurrent transitory ischemic hemiparesis. Acetylsalicylic acid and clopidogrel were subsequently administered. Severe nose bleeding occurred as a result of the medication inhibiting platelet aggregation.

The patient had to be intubated and ventilated. Endoscopy of the nasal cavity revealed that the tumor was bleeding. In fact, diffuse bleeding was found to originate from the surface of the nasopharyngeal fibroma on the nasal side. Platelets were infused into the patient. Standard gauze was soaked with epinephrine and applied on the tumor surface. Although blood loss could be significantly reduced, bleeding continued. The tumor surface was then covered with X-sponge, which immediately halted the bleeding.

The X-sponge packing was left in the nasal cavity and dissolved over the following two weeks without significant pain perception. Some parts of the sponge were discharged

from the nose. No further bleeding occurred after the primary intervention. The patient eventually underwent resection of the residual tumor mass.

The application of X-sponge in the nasal cavity was also documented in a 63-year old, male patient [Figure 7(B)]. The sponge was positioned between the lateral nasal wall and the middle turbinate. Rapid cessation of bleeding was achieved with X-sponge application in the anterior ethmoid after functional endoscopic sinus surgery.

### DISCUSSION

#### Hemostatic activity *in vitro*

Our *in vitro* data indicate that the novel gelatin-based sponge matrix has (a) a unique microstructure characterized by high porosity, (b) a high surface roughness in the nanorange, (c) accelerated blood absorption, and (d) rapid hemostasis in a venous hemorrhage model. We suspect that the structural matrix features could be the actual cause of the functional features that we observed.

Increased surface roughness is known to induce platelet adhesion and activation of the coagulating system.<sup>20,21</sup> Hovgaard et al.<sup>22</sup> demonstrated significant adsorption of proteins (especially of fibronectin) on surfaces with roughness on the nanoscale. Their data indicate that the nano roughness of the X-sponge might be one of the main features explaining the phenomenon of rapid hemostasis.

In our static model with hemostatic samples dipped into human blood, we observed extremely rapid blood uptake by the X-sponge. This phenomenon might be explained by the apparent increased capillary density and surface area of the sponge. As ongoing blood flow needs to be managed in the clinical setting, we also invented a dynamic model. Most intriguingly, we noted that in this hemorrhage model, hemostasis took effect two to three times faster than with other hemostyptic devices. An accelerated fluid flow tends to increase the shear stress inside the capillary network of the sponge. In turn, platelets might be activated more efficiently and consequently, coagulation might be accelerated.<sup>23-25</sup> Although this might explain some of the aspects identified in the hemorrhage model, we anticipate that additional mechanisms are at work to achieve the stunningly short time to complete hemostasis.

After exposure of the two different gelatin sponges to blood, electron micrographs revealed a fibrillar network which consisted of cells intertwined with elongated fibers characteristic of fibrin filaments. Most intriguing was the observation that the gelatin lamella surface was coated with irregular profiles, which presumably represented primary fibrin deposits. This feature was most pronounced on the X-sponge, which was characterized by a special surface roughness. Consequently, we hypothesize that the unique lamella surface provided more protein attachment sites. Though the X-sponge appeared to induce a more widespread formation of irregular profiles on its surfaces, it remains to be shown in the future whether the profiles detected by electron microscopy are indeed growing fibrin fibers. To emphasize the rapid blood absorption in conjunction with rapid

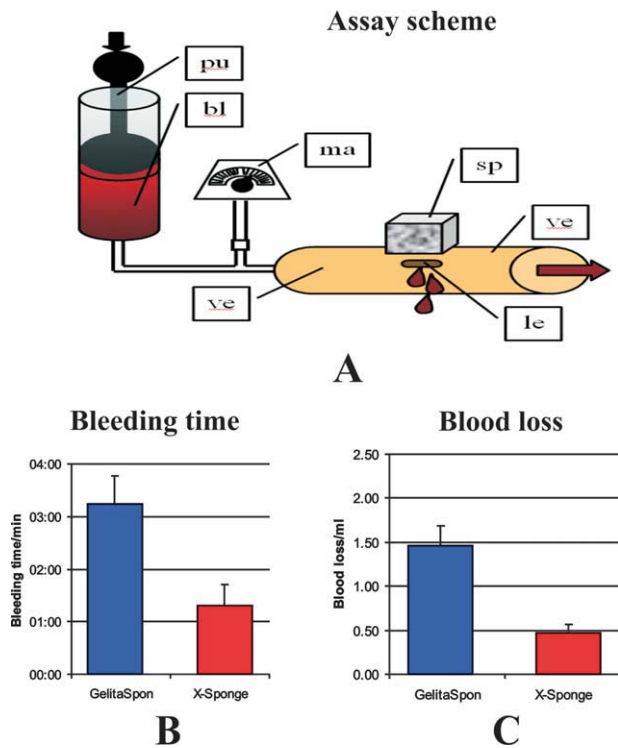


**FIGURE 6.** Hemostasis *in vitro*. Scheme of the experimental layout (A); bl, blood; ma, manometer; sp, test sponge; le, induced leak in the vessel; pu, pump; pr, pressure monitoring system; ve, human vein. The time to complete hemostasis after the application of different hemostyptic sponges was determined (B). Quantification of blood loss after the application of different hemostyptic sponges (C). X-sponge causes most rapid hemostasis. ( $n = 5$ ,  $**p < 0.05$ , SEM). [Color figure can be viewed in the online issue, which is available at [www.interscience.wiley.com](http://www.interscience.wiley.com).]

hemostasis, we apply the term “activated capillary function” to describe the X-sponge’s apparent mode of action.

### Hemostatic activity in humans

The first patient reported here who was treated with the X-sponge matrix was a child suffering from a tumor of the nasal cavity. After sinus surgery, nasal packs are used by ear-nose-throat (ENT) surgeons to achieve a hemostatic effect. The subsequent removal of nasal packs, however, may cause recurrent bleeding and pain. In recent years, a number of clinical trials have been performed, both testing the overall usefulness of nasal packs<sup>26,27</sup> and establishing criteria for a direct comparison between various products. In these trials, the investigators mostly focused on blood loss and pain as measured on an analog visual/subjective scale.<sup>28–31</sup>

It is worth noting that in some trials patients were specifically excluded from participation, if they were diagnosed with bleeding disorders or if anticoagulants, that is, agents inhibiting platelet aggregation, had been prescribed. However, this selected recruitment of patients for study enrollment does not reflect the typical clinical situation. It is common knowledge that there is an ever increasing number of patients who are diagnosed with coronary artery disease,

stroke and dysrhythmias, such as atrial fibrillation and for whom anticoagulants are prescribed.<sup>32–34</sup> In some patients, particularly those who have undergone a stenting procedure for coronary artery disease or carotid stenosis,<sup>35</sup> many physicians even consider double medication imperative, such as aspirin in combination with clopidogrel,<sup>36,37</sup> which on the one hand prevents stent thrombosis, but on the other hand puts the patients at increased risk for epistaxis.<sup>38,39</sup>

In ENT, the activated capillary function of the novel gelatin sponge matrix introduced here sets it apart from the traditional methods of nasal packing. In addition, most nasal packs need to be removed after surgery.<sup>15,40</sup> Removing and manipulating the tamponades may induce renewed bleeding<sup>41</sup> and can entail the formation of scar tissue, which in some cases eventually necessitates reoperation. In contrast, the bioresorbable, nontoxic gelatin matrix of X-sponge disintegrates completely within 14 days in the nasal cavity and is simply resorbed.

### Perspective

In summary, X-sponges are suitable for application in two situations, first, for the treatment of acute epistaxis, and second, as a hemostyptic device during surgical procedures, such as functional endoscopic sinus surgery and turbino-plasty. The novelty of this medical device lies in the fact that hemostasis is not only achieved by mechanical pressure but also by biophysical properties best described as activated capillary function, which brings about immediate hemostasis, particularly in patients treated with pharmacological agents inhibiting blood coagulation. Currently, the mechanism of gelatin-based hemostats is not fully understood.<sup>42</sup> Based on our *in vitro* data, we hypothesize that surface roughness and induced shear stress are possible factors in the accelerated hemostasis observed in X-sponge specimens. From the patient’s point of view, the discussed characteristics are associated with increased comfort. From the physician’s perspective, X-sponges facilitate patient management.

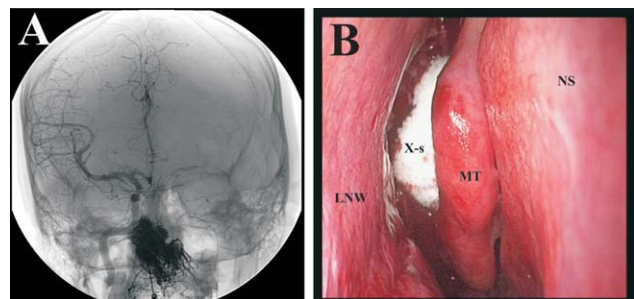


**FIGURE 7.** X-sponge application in human patients. Arterial angiography of the right internal carotid in a 12-year old male showing a highly vascularized tumor (arrow in A) situated along the pharyngeal wall (A). Application of X-sponge in a 63-old male in the anterior ethmoid after functional endoscopic sinus surgery (B). LNW, lateral nasal wall; MT, middle turbinate; NS, nasal septum; X, X-sponge. [Color figure can be viewed in the online issue, which is available at [www.interscience.wiley.com](http://www.interscience.wiley.com).]

## ACKNOWLEDGMENTS

The authors are grateful to Dr. S. Fennrich, Elvira Bublitz-Zaha, Norbert Kern, Clementine Warres, Elke Tetling, (all NMI, Reutlingen), Uwe Ahrweiler, Nida Berber, Heike Sych (all GELITA AG), Dr. Michael Schunck, and Anja Weber (CRI, Kiel) for experimental support, and D. Blaurock for correcting the manuscript.

## REFERENCES

- Sanghi P, Virmani R, Do D, Erikson J, Elliott J, Cilingiroglu M, Matthews H, Kazi M, Ricker R, Bayley SR. A comparative evaluation of arterial blood flow and the healing response after femoral artery closure using angio-seal STS Plus and StarClose in a porcine model. *J Interv Cardiol* 2008;21:329–336.
- Zirna H, Keating SE, Devincintis AF. Topical hemostatic agents to reduce bleeding from cancellous bone surfaces: A comparison of Gelfoam paste and bone wax. *J Foot Surg* 1987;26:496–500.
- Kastl KG, Betz CS, Siedek V, Leunig A. Control of bleeding following functional endoscopic sinus surgery using carboxy-methylated cellulose packing. *Eur Arch Otorhinolaryngol* 2009;266:1239–1243.
- Holcomb JB, Pusateri AE, Harris RA, Charles NC, Gomez RR, Cole JP, Beal LD, Bayer V, MacPhee MJ, Hess JR. Effect of dry fibrin sealant dressings versus gauze packing on blood loss in grade V liver injuries in resuscitated swine. *J Trauma* 1999;46:49–57.
- Kheirabadi BS, Acheson EM, Deguzman R, Sondeen JL, Ryan KL, Delgado A, Dick EJ, Jr, Holcomb JB. Hemostatic efficacy of two advanced dressings in an aortic hemorrhage model in Swine. *J Trauma* 2005;59:25–34.
- Pusateri AE, Holcomb JB, Harris RA, MacPhee MJ, Charles NC, Beall LD, Hess JR. Effect of fibrin bandage fibrinogen concentration on blood loss after grade V liver injury in swine. *Mil Med* 2001;166:217–222.
- Erdogan D, Van Gulik TM. Evolution of fibrinogen-coated collagen patch for use as a topical hemostatic agent. *J Biomed Mater Res B Appl Biomater* 2008;85:272–278.
- Walsh PN. Platelet coagulation-protein interactions. *Semin Thromb Hemost* 2004;30:461–471.
- Ahuja N, Ostomel TA, Rhee P, Stucky GD, Conran R, Chen Z, Al-Mubarak GA, Velmahos G, Demoya M, Alam HB. Testing of modified zeolite hemostatic dressings in a large animal model of lethal groin injury. *J Trauma* 2006;61:1312–1320.
- Arnaud F, Tomori T, Saito R, Mckeague A, Prusaczyk WK, Mccarroll RM. Comparative efficacy of granular and bagged formulations of the hemostatic agent QuikClot. *J Trauma* 2007;63:775–782.
- Carroway JW, Kent D, Young K, Cole A, Friedman R, Ward KR. Comparison of a new mineral based hemostatic agent to a commercially available granular zeolite agent for hemostasis in a swine model of lethal extremity arterial hemorrhage. *Resuscitation* 2008;78:230–235.
- Ward KR, Tiba MH, Holbert WH, Blocher CR, Draucker GT, Proffitt EK, Bowlin GL, Ivatury RR, Diegelmann RF. Comparison of a new hemostatic agent to current combat hemostatic agents in a Swine model of lethal extremity arterial hemorrhage. *J Trauma* 2007;63:276–283.
- Ellis-Behnke RG, Liang YX, Tay DK, Kau PW, Schneider GE, Zhang S, Wu W, So KF. Nano hemostat solution: immediate hemostasis at the nanoscale. *Nanomedicine* 2006;2:207–215.
- Lumsden AB, Heyman ER. Prospective randomized study evaluating an absorbable cyanoacrylate for use in vascular reconstructions. *J Vasc Surg* 2006;44:1002–1009.
- Gifford TO, Orlandi RR. Epistaxis. *Otolaryngol Clin North Am* 2008;41:525–536.
- Bugten V, Nordgard S, Skogvoll E, Steinsvag S. Effects of nonabsorbable packing in middle meatus after sinus surgery. *Laryngoscope* 2006;116:83–88.
- Orlandi RR, Lanza DC. Is nasal packing necessary following endoscopic sinus surgery? *Laryngoscope* 2004;114:1541–1544.
- Chandra RK, Kern RC. Advantages and disadvantages of topical packing in endoscopic sinus surgery. *Curr Opin Otolaryngol Head Neck Surg* 2004;12:21–26.
- Cansz H, Tahamiler R, Yener M, Acoglu E, Guvenc MG, Papila I, Sekercioglu N. Modified midfacial degloving approach for sino-nasal tumors. *J Craniofac Surg* 2008;19:1518–1522.
- Linneweber J, Dohmen PM, Kertzsch U, Affeld K, Nose Y, Konertz W. The effect of surface roughness on activation of the coagulation system and platelet adhesion in rotary blood pumps. *Artif Organs* 2007;31:345–351.
- Tsunoda N, Kokubo K, Sakai K, Fukuda M, Miyazaki M, Hiyoshi T. Surface roughness of cellulose hollow fiber dialysis membranes and platelet adhesion. *ASAIO J* 1999;45:418–423.
- Hovgaard MB, Rechendorff K, Chevallier J, Foss M, Besenbacher F. Fibronectin adsorption on tantalum: The influence of nano-roughness. *J Phys Chem B* 2008;112:8241–8249.
- Andrews RK, Berndt MC. Platelet adhesion: A game of catch and release. *J Clin Invest* 2008;118:3009–3011.
- Choi H, Aboulfatova K, Pownall HJ, Cook R, Dong JF. Shear-induced disulfide bond formation regulates adhesion activity of von Willebrand factor. *J Biol Chem* 2007;282:35604–35611.
- Ruggeri ZM, Orje JN, Habermann R, Federici AB, Reininger AJ. Activation-independent platelet adhesion and aggregation under elevated shear stress. *Blood* 2006;108:1903–1910.
- Awan MS, Iqbal M. Nasal packing after septoplasty: A randomized comparison of packing versus no packing in 88 patients. *Ear Nose Throat J* 2008;87:624–627.
- Dubin MR, Pletcher SD. Postoperative packing after septoplasty: Is it necessary? *Otolaryngol Clin North Am* 2009;42:279–285.
- Arya AK, Butt O, Nigam A. Double-blind randomized controlled trial comparing merocel with rapid rhino nasal packs after routine nasal surgery. *Rhinology* 2003;41:241–243.
- Bresnihan M, Mehigan B, Curran A. An evaluation of merocel and series 5000 nasal packs in patients following nasal surgery: A prospective randomized trial. *Clin Otolaryngol* 2007;32:352–355.
- Cruise AS, Amonoo-Kuofi K, Srouji I, Kanagalingam J, Georgalas C, Patel NN, Badia L, Lund VJ. A randomized trial of Rapid Rhino Riemann and Telfa nasal packs following endoscopic sinus surgery. *Clin Otolaryngol* 2006;31:25–32.
- Prabhu V, Kaushik V, Rhodes S, Tay H. Foam nasal packs: A prospective, randomized, patient-controlled study. *Rhinology* 2007;45:242–247.
- Boussier MG. Antithrombotic agents in the prevention of ischemic stroke. *Cerebrovasc Dis* 2009;27 (Suppl 3):12–19.
- Crandall MA, Bradley DJ, Packer DL, Asirvatham SJ. Contemporary management of atrial fibrillation: Update on anticoagulation and invasive management strategies. *Mayo Clin Proc* 2009;84:643–662.
- Leys D, Balucani C, Cordonnier C. Antiplatelet drugs for ischemic stroke prevention. *Cerebrovasc Dis* 2009;27 (Suppl 1):120–125.
- Liapis CD, Bell PR, Mikhailidis D, Sivenius J, Nicolaidis A, Fernandes E, Fernandes J, Biasi G, Norgren L. ESVS Guidelines Collaborators. Invasive treatment for carotid stenosis: Indications, techniques. *Eur J Vasc Endovasc Surg* 2009;37 (Suppl):1–19.
- Holmes DR, Kereiakes DJ, Kleiman NS, Moliterno DJ, Patti G, Grines CL. Combining antiplatelet and anticoagulant therapies. *J Am Coll Cardiol* 2009;54:95–109.
- Vande Griend JP, Saseen JJ. Combination antiplatelet agents for secondary prevention of ischemic stroke. *Pharmacotherapy* 2008;28:1233–1242.
- Rainsbury JW, Molony NC. Clopidogrel versus low-dose aspirin as risk factors for epistaxis. *Clin Otolaryngol* 2009;34:232–235.
- Cohen M. Expanding the recognition and assessment of bleeding events associated with antiplatelet therapy in primary care. *Mayo Clin Proc* 2009;84:149–160.
- Hajioannou JK, Bizaki A, Fragiadakis G, Bourolia C, Spanakis I, Chlouverakis G, et al. Optimal time for nasal packing removal after septoplasty. A comparative study. *Rhinology* 2007;45:68–71.
- Mathiasen RA, Cruz RM. Prospective, randomized, controlled clinical trial of a novel matrix hemostatic sealant in patients with acute anterior epistaxis. *Laryngoscope* 2005;115:899–902.
- Seyednejad H, Imani M, Jamieson T, Seifalian AM. Topical haemostatic agents. *Br J Surg* 2008;95:1197–1225.